

Advancing the State-of-the-Art for ECG Analysis through Structured State Space Models

Temesgen Mehari

*Physikalisch-Technische Bundesanstalt, Berlin, Germany
Fraunhofer Heinrich-Hertz-Institut, Berlin, Germany*

TEMESGEN.MEHARI@PTB.DE

Nils Strodthoff

Carl von Ossietzky Universität Oldenburg, Oldenburg, Germany

NILS.STRODTHOFF@UNI-OLDENBURG.DE

Abstract

The field of deep-learning-based ECG analysis has been largely dominated by convolutional architectures. This work explores the prospects of applying the recently introduced structured state space models (SSMs) as a particularly promising approach due to its ability to capture long-term dependencies in time series. We demonstrate that this approach leads to significant improvements over the current state-of-the-art for ECG classification, which we trace back to individual pathologies. Furthermore, the model's ability to capture long-term dependencies allows to shed light on long-standing questions in the literature such as the optimal sampling rate or window size to train classification models. Interestingly, we find no evidence for using data sampled at 500Hz as opposed to 100Hz and no advantages from extending the model's input size beyond 3s. Based on this very promising first assessment, SSMs could develop into a new modeling paradigm for ECG analysis.

Keywords: Cardiology, Electrocardiography (ECG), Time series classification, Structured state space models

1. Introduction

Machine learning and deep learning in particular deep learning has the potential to trans-

form the entire field of healthcare. The electrocardiogram (ECG) is particularly suited to spearhead this development due to its widespread use (in the US during about 5% of the office visits, an ECG was ordered or provided (CDC, 2019)). While it only requires basic recording equipment, it holds enormous diagnostic potential that we only gradually start to uncover assisted by machine learning (Hannun et al., 2019a; Attia et al., 2019; Lima et al., 2021; Verbrugge et al., 2022). On the algorithmic side, the analysis of ECGs based on raw sensor data is still largely dominated by convolutional neural networks (Strodthoff et al., 2020; Hannun et al., 2019b; Attia et al., 2019; Ribeiro et al., 2020). This default choice is slowly challenged by the rise of transformer-based architectures or combinations of convolutional architectures with attention elements as exemplified by the winning solutions of the two past editions of the Computing in Cardiology Challenge (Natarajan et al., 2020; Nejedly et al., 2021). In this work, we explore a novel algorithmic approach, *Structured State Space Sequence (S₄) Models* (Gu et al., 2022a), which learns a continuous representation of time series data and are particularly suited for modeling long-term dependencies.

We put the model through a thorough evaluation using an established benchmarking procedure (Strodthoff et al., 2020) on the

PTB-XL (Wagner et al., 2020a,b; Goldberger et al., 2000) and *Chapman* (Zheng et al., 2020) datasets demonstrating consistent improvements over the existing (mostly convolutional) state-of-the-art methods on both datasets, which we trace back to improvements in the predictive performance for individual ECG statements.

We demonstrate the model’s ability for evaluation at sampling rates unseen during training, essentially without any loss in predictive performance. Furthermore, we use the model capability to capture long-term dependencies to systematically investigate several long-standing questions in the field, i.e. how long-ranged are interactions in ECG data that have to be captured explicitly by the model and do models actually profit from input data at a sampling frequency of 500 Hz as compared to 100 Hz.

2. Related Work

ECG classification The field of ECG analysis is largely dominated by convolutional architectures, see (Hong et al., 2020; Petmezas et al., 2022) for a recent reviews. The superiority of modern ResNet- or Inception-based convolutional architectures was confirmed in an extensive comparative study on the *PTB-XL* dataset (Strodthoff et al., 2020). This is in line with the excellent performance of such architectures on a broad range of time series classification tasks, see (Ismail Fawaz et al., 2020). Interestingly, this supremacy was already challenged in (Mehari and Strodthoff, 2022), where the convolutional baseline was outperformed by a large recurrent neural network with convolutional feature extractor. Therefore, it represents a natural question to ask whether architectures that are even more adapted to the necessities of time series can lead to further performance improvements.

Structured State Space Models for clinical time series The motivation for the

development of structured state space models (SSMs) was the wish to devise an architecture that is suited to capture long-term dependencies in very long temporal data, including medical time series as a particular example (Gu et al., 2021). To support the applicability to the latter, the authors considered a classical vital sign prediction task on ECG and PPG time series as input (Gu et al., 2021, 2022b) and clearly outperformed the current state-of-the-art for this tasks. These results represent a very encouraging sign for the application of these models in the broader context of medical time series. Nevertheless the prior study cannot be considered as a comprehensive ECG analysis task, which is the topic of this work. In a different line of work, SSMs were used to model the internal state in diffusion models for time series imputation (Alcaraz and Strodthoff, 2022), which lead to unprecedented imputation quality (among others) for ECG data, which provides additional hints for the potential advantages of SSMs also in a purely discriminative setting. We therefore aim to investigate the motivating claims for SSMs in the context of ECG data.

3. Methods

3.1. Models

Structured State Space Models Structured State Space Models (SSMs) were introduced in (Gu et al., 2022a) showing outstanding results on problems that require capturing long-range dependencies. The model consists of stacked S_4 layers that in turn draw on state-space models, frequently used in control theory, of the form

$$\begin{aligned} x'(t) &= \mathbf{A}x(t) + \mathbf{B}u(t), \\ y(t) &= \mathbf{C}x(t) + \mathbf{D}u(t), \end{aligned} \tag{1}$$

that map a one-dimensional input $u(t) \in \mathbb{R}$ to a one-dimensional output $y(t) \in \mathbb{R}$ mediated through a hidden state $x(t) \in \mathbb{R}^N$

parametrized through matrices A, B, C, D . These continuous-time parameters can be mapped to discrete-time parameters $\bar{A}, \bar{B}, \bar{C}$ for a given step size Δ . These allow to form the *SSM convolutional kernel* $\bar{K}(\bar{A}, \bar{B}, \bar{C})$ that allows to calculate the output y by a simple convolution operation, $y = \bar{K} * u$. One of the main contribution of (Gu et al., 2022a) lies in providing a stable and efficient way to evaluate the kernel \bar{K} . Second, building on earlier work (Gu et al., 2020), they identify a particular way, according to HiPPO theory (Gu et al., 2020), of initializing the matrix $A \in \mathbb{R}^{n \times n}$ as key to capture long-range interactions. H copies of such layers parameterizing a mapping from $\mathbb{R} \rightarrow \mathbb{R}$ are now concatenated and fused through a point-wise linear operation to form a S4 layer mapping from $\mathbb{R}^H \rightarrow \mathbb{R}^H$.

Supervised model The model used for supervised training follows the original S4 architecture (Gu et al., 2022a) and consists of a convolutional layer as input encoder, followed by four *S4 blocks* which are connected through residual connections interleaved with normalization layers, with a global pooling layer and a linear classifier on top. The S4 blocks comprise the S4 layer accompanied by dropout and GeLU activations and a linear layer, see (Gu et al., 2022a) for details. The architecture is summarized schematically in Fig. A.1. We use the shorthand notation *4S4+1FC* to refer to this model.

3.2. Datasets and experimental procedure

To benchmark the performance of the proposed approach, we use two large, publicly available 12-lead ECG datasets, namely the *PTB-XL* (Wagner et al., 2020a,b; Goldberger et al., 2000) and the *Chapman* (Zheng et al., 2020) datasets. For *PTB-XL*, we follow the benchmarking methodology established in

(Strodthoff et al., 2020) and report the performance in terms of macro AUC (on the test fold) on the most finegrained level with 71 labels covering a broad range of diagnostic, form-related and rhythm-related ECG statements. For *Chapman*, we use the rhythm statements provided as primary annotations in the dataset. We mimic the procedure followed on *PTB-XL* as closely as possible by forming 10 stratified folds (8 training, 1 validation, 1 test fold) and also use macro AUC as performance metric. To ensure that each fold contains at least one sample of each ECG statement, we filter out statements that occur fewer than ten times. This reduces the label set from 68 to 48 statements.

For the experiments involving S4 layers, we use a batch size of 32, $N = 8$ for the state dimension in the S4-Layers (as optimal value identified on the *PTB-XL* validation set) and train the model with a constant learning rate schedule and a learning rate $lr = 0.001$ for 50 epochs with the AdamW Optimizer (Loshchilov and Hutter, 2017). If not stated otherwise, we train models on input sequences of length 2.5s in order to remain comparability to results in the literature. During training, subsequences are randomly cropped from the input record. During test time, we use test-time-augmentation: We create ten overlapping crops of the same length as the input size used during training from the original record, using different strides such that the whole sample gets covered, and take the mean of their respective output probabilities as final prediction for the entire sample.

4. Results

SSMs outperform the current supervised state-of-the-art As mentioned above, state-of-the-art approaches in deep-learning-based ECG analysis mainly rely on modern convolutional architectures. As a

representative example, we use a model with *xresnet1d50* architecture that was shown to lead to competitive results compared to the state-of-the-art at that time (Mehari and Strodthoff, 2022). We also compare to a recurrent neural network with convolutional feature extractor (*4FC+2LSTM+2FC*) (Mehari and Strodthoff, 2022) that showed the best reported supervised performance on *PTB-XL* to date. In Table 1, we compare these models to the *4S4+1FC* model based on comprehensive ECG classification tasks on the *PTB-XL* and *Chapman* datasets. On *PTB-XL*, the *4S4+1FC* model outperforms all baseline methods in a statistically significant manner, see below for a detailed description. Interestingly, the ranking of the algorithms is largely consistent on the *Chapman* dataset but the differences between the different approaches are not significant in this case. This might be explained by the fact that all models achieve very high predictive performance on this dataset with macro AUC values beyond 0.98, which is not the ideal situation if one aims to quantify performance differences in a statistically significant manner.

For a proper discussion of the results, we have to refine our notion of statistical and systematical uncertainty measures. Following the methodology used in (Mehari and Strodthoff, 2022), we consider two sources of uncertainty, the statistical uncertainty due to the randomness of the training process, which can be assessed through multiple training runs, and the uncertainty due to the finiteness and the specificity of the label distribution of the test set. We address the latter via empirical bootstrapping ($n_{\text{iter}} = 1000$ iterations) on the test set. Comparing two particular trained models, we consider the performance difference to be statistically significant if the bootstrap 95% confidence intervals for the performance difference does not overlap with zero. We

address the uncertainty due to the stochasticity of the training process by training $n_{\text{runs}} = 10$ for each of the models we aim to compare. For each of the n_{runs}^2 comparisons, we assess the statistical significance via bootstrapping as defined above. Finally, we define a model to perform statistically significantly better/worse in case that 60% of the model comparisons turn out to be statistically significantly better/worse. Just like the significance level, this threshold can be chosen at will as long as it exceeds 40% for consistency reasons (Springenberg et al., 2022) and relates to the amount of uncertainty due to fluctuations across training runs one is willing to tolerate.

Furthermore, in Appendix B, we look into specific pathologies to investigate whether or to what extent the improved performance of the *4S4+1FC* model can be traced back to certain pathologies. Summarizing, we find statistical significant improvements for 8 (SARRH, PAC, ISCIN,STD-, ABQRS, SR, IMI, NORM) of the 71 ECG statements, while only for 2AVB the performance decreased consistently.

SSMs allow inference at unseen sampling rates A compelling aspect of state space models is that, due to the continuous character of the state-transition matrix \mathbf{A} in equation 1, the model can be evaluated on data that was sampled at a different rate than the training data, by simply adjusting the step size in the discretization step during test time. Table 2 depicts a cross-evaluation matrix, in which we trained and cross-evaluated the *4S4+1FC* model on 100, 200 and 500Hz. We see no or just minor losses in performance when varying test from train sampling rates, even if the sampling rates differ by a factor of 5. This is a particular asset of SSM models as it avoids the necessity to resample the data, which might otherwise be a source of additional systematic uncertainties.

Table 1: Comparing supervised performance of the state-of-the-art models on two large ECG datasets. Here and in the following, we report mean and standard deviation of the test set scores over 10 runs using a concise error notation where e.g. $0.9175(39)$ signifies 0.9175 ± 0.0039 . The asterisks stands for statistically significant better performance than $4FC+2LSTM+2FC$ (as the previous state-of-the-art).

	dataset	
	<i>PTB-XL</i>	<i>Chapman</i>
<i>xresnet1d50</i> (Strodthoff et al., 2020)	0.9286(28)	0.9805(39)
$4FC+2LSTM+2FC$ (causal) (Mehari and Strodthoff, 2022)	0.9295(31)	0.9854(12)
$4S_4+1FC$ (this work)	0.9417(16)*	0.9876(11)

Table 2: Comparing supervised performance of the $4S_4+1FC$ model trained/tested on different sampling rates.

		test		
		100Hz	200Hz	500Hz
train	100Hz	0.9417(35)	0.9418(36)	0.9416(36)
	200Hz	0.9414(16)	0.9416(16)	0.9417(16)
	500Hz	0.9415(18)	0.9421(19)	0.9421(19)

No long-term dependencies in ECG data beyond 3s In this paragraph, we aim to clarify in a quantitative way, how long-ranged interactions are actually present in ECG data, which is a long-standing question that has not been systematically addressed so far. We address this question in terms of the size of the input window that is passed to the model (while performing test-time-augmentation, i.e. combining information from different segments for the sample-level prediction at all times). We believe that this question could not be answered in an unbiased way so far due to the inability of prior architectures to capture long-term dependencies in the data without adjusting hyperparameters such as kernel sizes etc. in the case of convolutional models. In Fig. 4, we investigate the model performance (macro AUC measured on the *PTB-XL* test set) as

a function of input size for two convolutional models using input data sampled at 100Hz and 500Hz and two SSMs using the same kind of input data. As described above, we train models on various input sizes, measured in physical units for comparability, and obtain aggregated predictions for the full samples during test time by taking the average of ten input windows that are consequently moved through the signal with varying stride. As first observation from Fig. 4, we see that the performance gap between convolutional models and structured state space models, which was already apparent at an input size of 2.5s in Tab. 1, persists across all input sizes. Second, within each model architecture, the results from input data sampled at 100Hz as compared to 500Hz largely overlap. This already puts into question the potential advantage of using input data at

500Hz for ECG classification purposes. We will revisit this question in a more detail in the next paragraph. Third, the plot shows an interesting dependence on the input size that is qualitatively consistent across model architectures: The performance from aggregated model predictions shows a peak around input sizes around 2-3s. This hints at the fact that for ECG classification tasks based on short 12-lead ECG data, the ability of the model to explicitly capture long-range interactions beyond about 3s is not beneficial. On the contrary, the models seems to profit more from averaging overlapping predictions from different sliding windows. This observation is very much in line with the fact that most pathologies affect all beats equally (with a few exceptions such as premature ventricular contractions) and the fact that for average heart rates between 60 and 100bpm, a sliding window of 3s already contains 3-5 beats. This question is obviously completely independent from the question of capturing long-term dependencies in long-term ECGs with potentially rapid rhythm changes within the sample and should be revisited in this context in future work.

No significant advantages from sampling frequencies beyond 100Hz We also revisit the question of the comparison between sampling frequencies at 100Hz vs. 500Hz in a statistically more rigorous manner based on the methodology presented above. At a input size of 2.5s and for fixed model architecture, we find no statistically significant performance difference between both sampling frequencies. This applies equally well to the level of individual label AUCs, in an analysis analogous to the one carried out for the comparison between 4S4+1FC and xresnet above. We want to stress that this statement obviously strongly depends on the label distribution of the dataset under consideration in the sense that there might be systematic im-

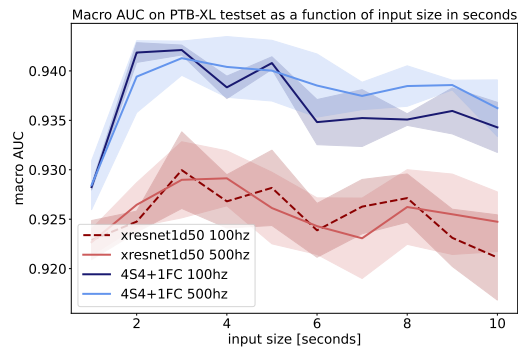


Figure 1: Model performance in dependence of (physical) input size for two convolutional models (*xresnet1d50*) at 100/500Hz as compared to two SSMs (4S4+1FC) at 100/500Hz.

provements for certain ECG statements that do not turn out to be statistically significant due to large fluctuations as a consequence of small samples sizes.

5. Summary

In this work, we used structured state space models, which are particularly suited to capture long-term dependencies in time series, to challenge the supremacy of convolutional architectures in the field of deep-learning-based ECG analysis. In fact, we were able to demonstrate consistent improvements over the previous state-of-the-art on large, comprehensive ECG classification datasets. We use the model’s ability to capture long-term dependencies to shed new light on the question of the optimal sampling frequency and the model’s input size. The code underlying our experiments is publicly available under https://github.com/tmehari/ssm_ecg.

Acknowledgments

This project (18HLT07 MedalCare) has received funding from the EMPIR programme co-financed by the Participating States and from the European Union’s Horizon 2020 research and innovation programme.

References

- Juan Miguel Lopez Alcaraz and Nils Strodthoff. Diffusion-based time series imputation and forecasting with structured state space models. *arXiv preprint 2208.09399*, 2022.
- Zachi I. Attia, Suraj Kapa, Francisco Lopez-Jimenez, Paul M. McKie, Dorothy J. Ladewig, Gaurav Satam, Patricia A. Pellikka, Maurice Enriquez-Sarano, Peter A. Noseworthy, Thomas M. Munger, Samuel J. Asirvatham, Christopher G. Scott, Rickey E. Carter, and Paul A. Friedman. Screening for cardiac contractile dysfunction using an artificial intelligence-enabled electrocardiogram. *Nature Medicine*, 25(1):70–74, January 2019. doi: 10.1038/s41591-018-0240-2.
- CDC. National Ambulatory Medical Care Survey: 2016 National Summary Tables. Technical report, Centers for Disease Control and Prevention, 2019.
- Ary L. Goldberger, Luis A. N. Amaral, Leon Glass, Jeffrey M. Hausdorff, Plamen Ch. Ivanov, Roger G. Mark, Joseph E. Mietus, George B. Moody, Chung-Kang Peng, and H. Eugene Stanley. PhysioBank, PhysioToolkit, and PhysioNet. *Circulation*, 101(23):e215–e220, 2000. doi: 10.1161/01.CIR.101.23.e215.
- Albert Gu, Tri Dao, Stefano Ermon, Atri Rudra, and Christopher Ré. Hippo: Recurrent memory with optimal polynomial projections. In H. Larochelle, M. Ranzato, R. Hadsell, M.F. Balcan, and H. Lin, editors, *Advances in Neural Information Processing Systems*, volume 33, pages 1474–1487. Curran Associates, Inc., 2020.
- Albert Gu, Isys Johnson, Karan Goel, Khaled Saab, Tri Dao, Atri Rudra, and Christopher Ré. Combining recurrent, convolutional, and continuous-time models with linear state space layers. In M. Ranzato, A. Beygelzimer, Y. Dauphin, P.S. Liang, and J. Wortman Vaughan, editors, *Advances in Neural Information Processing Systems*, volume 34, pages 572–585. Curran Associates, Inc., 2021.
- Albert Gu, Karan Goel, and Christopher Ré. Efficiently modeling long sequences with structured state spaces. In *International Conference on Learning Representations*, 2022a.
- Albert Gu, Ankit Gupta, Karan Goel, and Christopher Ré. On the parameterization and initialization of diagonal state space models. *arXiv preprint 2206.11893*, 2022b.
- Awni Y. Hannun, Pranav Rajpurkar, Mousoumeh Haghpanahi, Geoffrey H. Tison, Codie Bourn, Mintu P. Turakhia, and Andrew Y. Ng. Cardiologist-level arrhythmia detection and classification in ambulatory electrocardiograms using a deep neural network. *Nature Medicine*, 25(1):65–69, January 2019a. doi: 10.1038/s41591-018-0268-3.
- Awni Y. Hannun, Pranav Rajpurkar, Mousoumeh Haghpanahi, Geoffrey H. Tison, Codie Bourn, Mintu P. Turakhia, and Andrew Y. Ng. Cardiologist-level arrhythmia detection and classification in ambulatory electrocardiograms using a deep neural network. *Nature Medicine*, 25(1):65–69, 2019b. doi: 10.1038/s41591-018-0268-3.
- Shenda Hong, Yuxi Zhou, Junyuan Shang, Cao Xiao, and Jimeng Sun. Opportuni-

- ties and challenges of deep learning methods for electrocardiogram data: A systematic review. *Computers in Biology and Medicine*, 122:103801, July 2020. doi: 10.1016/j.compbiomed.2020.103801.
- Hassan Ismail Fawaz, Benjamin Lucas, Germain Forestier, Charlotte Pelletier, Daniel F. Schmidt, Jonathan Weber, Geoffrey I. Webb, Lhassane Idoumghar, Pierre-Alain Muller, and François Petitjean. Inceptiontime: Finding alexnet for time series classification. *Data Mining and Knowledge Discovery*, 2020.
- Emilly M. Lima, Antônio H. Ribeiro, Gabriela M. M. Paixão, Manoel Horta Ribeiro, Marcelo M. Pinto-Filho, Paulo R. Gomes, Derick M. Oliveira, Ester C. Sabino, Bruce B. Duncan, Luana Giatti, Sandhi M. Barreto, Wagner Meira Jr, Thomas B. Schön, and Antonio Luiz P. Ribeiro. Deep neural network-estimated electrocardiographic age as a mortality predictor. *Nature Communications*, 12(1), August 2021. doi: 10.1038/s41467-021-25351-7.
- Ilya Loshchilov and Frank Hutter. Decoupled weight decay regularization. In *International Conference on Learning Representations*, 2017.
- Temesgen Mehari and Nils Strodthoff. Self-supervised representation learning from 12-lead ECG data. *Computers in Biology and Medicine*, 141:105114, February 2022. doi: 10.1016/j.compbiomed.2021.105114.
- Annamalai Natarajan, Yale Chang, Sara Mariani, Asif Rahman, Gregory Boverman, Shruti Vij, and Jonathan Rubin. A wide and deep transformer neural network for 12-lead ecg classification. In *2020 Computing in Cardiology (CinC)*. IEEE, 2020. doi: 10.22489/CinC.2020.107.
- Petr Nejedly, Adam Ivora, Radovan Smisek, Ivo Viscor, Zuzana Koscova, Pavel Jurak, and Filip Plesinger. Classification of ECG using ensemble of residual CNNs with attention mechanism. In *2021 Computing in Cardiology (CinC)*. IEEE, September 2021. doi: 10.23919/cinc53138.2021.9662723.
- Georgios Petmezas, Leandros Stefanopoulos, Vassilis Kilintzis, Andreas Tzavelis, John A Rogers, Aggelos K Katsaggelos, Nicos Maglaveras, et al. State-of-the-art deep learning methods on electrocardiogram data: Systematic review. *JMIR medical informatics*, 10(8):e38454, 2022.
- Antônio H. Ribeiro, Manoel Horta Ribeiro, Gabriela M. M. Paixão, Derick M. Oliveira, Paulo R. Gomes, Jéssica A. Canazart, Milton P. S. Ferreira, Carl R. Andersson, Peter W. Macfarlane, Meira Wagner, Thomas B. Schön, and Antonio Luiz P. Ribeiro. Automatic diagnosis of the 12-lead ECG using a deep neural network. *Nature Communications*, 11(1), April 2020. doi: 10.1038/s41467-020-15432-4.
- Maximilian Springenberg, Annika Frommholz, Markus Wenzel, Eva Weicken, Jackie Ma, and Nils Strodthoff. From cnns to vision transformers – a comprehensive evaluation of deep learning models for histopathology. *arXiv preprint 2204.05044*, 2022.
- Nils Strodthoff, Patrick Wagner, Tobias Schaeffter, and Wojciech Samek. Deep learning for ecg analysis: Benchmarks and insights from ptb-xl. *IEEE Journal of Biomedical and Health Informatics*, 25(5): 1519–1528, 2020.
- Frederik H. Verbrugge, Yogesh N.V. Reddy, Zachi I. Attia, Paul A. Friedman, Peter A. Noseworthy, Francisco Lopez-

Jimenez, Suraj Kapa, and Barry A. Borlaug. Detection of left atrial myopathy using artificial intelligence-enabled electrocardiography. *Circulation: Heart Failure*, 15(1), January 2022. doi: 10.1161/circheartfailure.120.008176.

Patrick Wagner, Nils Strodthoff, Ralf-Dieter Bousseljot, Dieter Kreiseler, Fatima I. Lunze, Wojciech Samek, and Tobias Schaeffter. PTB-XL, a large publicly available electrocardiography dataset. *Scientific Data*, 7(1):154, 2020a. doi: 10.1038/s41597-020-0495-6.

Patrick Wagner, Nils Strodthoff, Ralf-Dieter Bousseljot, Wojciech Samek, and Tobias Schaeffter. PTB-XL, a large publicly available electrocardiography dataset, 2020b.

Jianwei Zheng, Jianming Zhang, Sidy Danioko, Hai Yao, Hangyuan Guo, and Cyril Rakovski. A 12-lead electrocardiogram database for arrhythmia research covering more than 10, 000 patients. *Scientific Data*, 7(1), February 2020. doi: 10.1038/s41597-020-0386-x.

Appendix A. Datasets & Models

Table A.1 summarizes the datasets used in this study and Figure A.1 presents the used model architecture.

Appendix B. Bootstrap Comparison on pathology Level

In Figure B.1, we show a bootstrap comparison between the $4S_4+1FC$ architecture and the *xresnet1d50* architecture on the level of individual ECG statements. The colored bars represent the median values and the black bars the standard deviation of the n_{runs}^2 medians of the n_{iter} AUC difference comparisons per model combination. Labels on

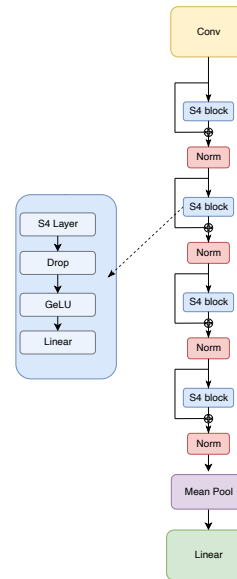


Figure A.1: The model used during supervised training follows the original S4 architecture (Gu et al., 2022a). The model consists of a convolutional layer as input encoder, followed by four S4 blocks which are connected through residual connections with a normalization layer. The prediction is obtained from a linear layer following a mean pooling layer.

Table A.1: Overview over the datasets used in this study.

dataset	# samples
Evaluation/Supervised training	
<i>PTB-XL</i> (Wagner et al., 2020a)	21,837
<i>Chapman</i> (Zheng et al., 2020)	10,646

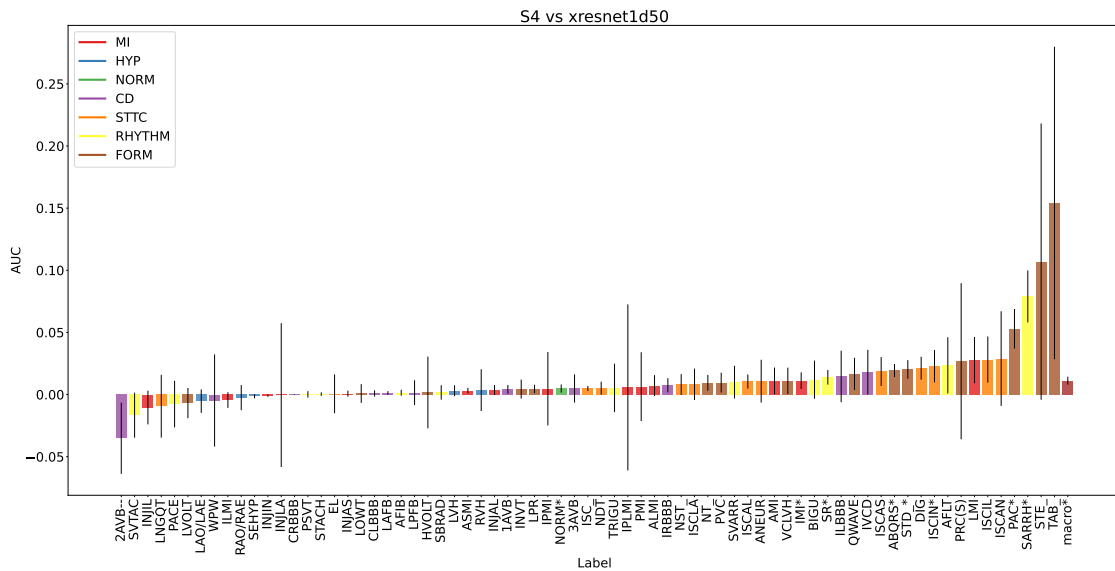


Figure B.1: Comparison of $4S4+1FC$ and *xresnet1d50* model performance at sampling rate 100Hz. We plot label $AUC(4S4+1FC)$ -label $AUC(xresnet1d50)$. The asterisk means that the $4S4+1FC$ model performs statistically significantly better and – that it performs statistically significantly worse than the *xresnet1d50* model on the respective label.

which the $4S_4+1FC$ architecture performs statistically better(worse) are marked by $*$ ($-$). The plot reveals that despite high median values for the difference of some label AUCs, like e.g for non-specific ST Elevation (STE) or T-wave abnormality (TAB), the $4S_4+1FC$ architecture does not necessarily perform statistically better on those labels, as the difference varies strongly over combinations of different runs. On the other hand though, there are pathologies, where the median AUC difference is close to zero but with such a low variance, that these differences are statistically significant, as it is the case for e.g. healthy ecg signals (NORM) or inferior myocardial infarctions (IMI).